Mutations in a gene encoding a midbody kelch protein in familial and sporadic classical Hodgkin lymphoma lead to binucleated cells

Stephen J. Salipante[a], Matthew E. Mealiffe[b,1], Jeremy Wechsler[c], Maxwell M. Krem[d], Yajuan Liu[b], Shinae Namkoong[b], Govind Bhagat[e], Tomas Kirchhoff[f], Kenneth Offit[f], Henry Lynch[g], Peter H. Wiernik[h], Mikhail Roshal[i], Mary Lou McMaster[j], Margaret Tucker[j], Jonathan R. Fromm[i], Lynn R. Goldin[j], and Marshall S. Horwitz[c,2]

[a]Department of Genome Sciences, [b]Division of Medical Genetics, Department of Medicine, [c]Department of Pathology, [d]Medical Oncology Program, [i]Department of Laboratory Medicine, University of Washington School of Medicine, Seattle, WA 98195; [e]Department of Pathology, College of Physicians and Surgeons of Columbia University, New York, NY 10032; [f]Memorial Sloan-Kettering Cancer Center, Clinical Cancer Genetics Laboratory, New York, NY 10065; [g]Department of Preventive Medicine, Creighton University School of Medicine, Omaha, NE 68178; [h]Our Lady of Mercy Cancer Center, New York Medical College, Bronx, NY 10466; and [j]Genetic Epidemiology Branch, Division of Cancer Epidemiology and Genetics, National Cancer Institute, Bethesda, MD 20892

Edited by Mary-Claire King, University of Washington, Seattle, WA, and approved July 2, 2009 (received for review April 16, 2009)

Classical Hodgkin lymphoma (cHL) is a malignancy of B-cell origin in which the neoplastic cells, known as ''Reed-Sternberg'' (RS) cells, are characteristically binucleated. Here we describe a family where multiple individuals developing cHL have inherited a reciprocal translocation between chromosomes 2 and 3. The translocation disrupts *KLHDC8B*, an uncharacterized gene from a region (3p21.31) previously implicated in lymphoma and related malignancies, resulting in its loss of expression. We tested *KLHDC8B* as a candidate gene for cHL and found that a 5′-UTR polymorphism responsible for decreasing its translational expression is associated with cHL in probands from other families with cHL and segregates with disease in those pedigrees. In one of three informative sporadic cases of cHL, we detected loss of heterozygosity (LOH) for *KLHDC8B* in RS cells, but not reactive T lymphocytes, purified from a malignant lymph node. *KLHDC8B* encodes a protein predicted to contain seven kelch repeat domains. KLHDC8B is expressed during mitosis, where it localizes to the midbody structure connecting cells about to separate during cytokinesis, and it is degraded after cell division. Depletion of KLHDC8B through RNA interference leads to an increase in binucleated cells, implicating its reduced expression in the formation of cHL's signature RS cell.

cancer | cytokinesis

Classical Hodgkin lymphoma (cHL) (1) is a lymph node cancer of germinal center B-cell origin. cHL tumors consist of a minority of malignant ''Reed-Sternberg'' (RS) cells mixed with reactive lymphocytes and other benign inflammatory cells. A defining feature of RS cells is the presence of two nuclei. cHL, along with nasopharyngeal carcinoma and a few other malignancies, is associated with Epstein-Barr virus (EBV) exposure (2), but genetic factors also contribute to risk.

In fact, the familial risk for cHL is very high. The risk in first degree relatives of cases is elevated 3- to 4-fold compared with the general population; the risk is greater still when onset of cHL in the proband is under age 40 (3). A recent genome-wide scan detected multiple loci possibly linked to familial cHL (4), indicating that genetic heterogeneity may pose a challenge for the identification of cHL susceptibility genes through a linkage-based strategy. Chance ascertainment of rare families cosegregating chromosomal abnormalities remains an established paradigm for disease gene identification, however, and was the approach that initially led to discovery of tumor suppressor genes responsible for retinoblastoma (5) and familial adenomatous polyposis (6), among other types of cancer.

Here we report a family where several individuals carrying a constitutional translocation involving chromosomes 2 and 3 have developed cHL. Intriguingly, the breakpoint on chromosome 3 is situated in a region (3p21.31) where frequent somatic cytogenetic rearrangements have been observed for both cHL and nonHodgkin lymphoma (7). Additionally, genetic linkage analysis (8), chromosome transfer experiments (9), and loss of heterozygosity (LOH) studies (10) have also implicated 3p21.31 in nasopharyngeal carcinoma, which shares an association with EBV. Moreover, 3p21.31 LOH is common in breast cancer (11), and breast cancer occurs more often among first degree relatives of cHL patients than in the general population (3). We therefore proceeded to molecularly define the translocation to determine if it disrupts a gene that may contribute to development of cHL and other forms of cancer.

Results

Description of the Family. In this pedigree (Fig. 1*A*), cHL has occurred in conjunction with a constitutional chromosomal abnormality. The proband developed the nodular sclerosis type of cHL at age 39. Two siblings also developed nodular sclerosis cHL as adults. Their mother died shortly after presenting with a mediastinal tumor (which is compatible with cHL, based on its location), for which she declined workup. A maternal first cousin succumbed to a brainstem tumor (which was probably not cHL, because it is only rarely found here). Individuals with cancer for whom genetic material is available or for whom karyotype can be inferred inherited a t(2,3) (q11.2;p21.31) translocation (Fig. 1*B*).

Mapping the 3p21.31 Translocation Breakpoint within *KLHDC8B*. We initially used fluorescence in situ hybridization (FISH) to map bacterial artificial chromosomes (BACs) spanning the breakpoints, as revealed by "split" signals appearing on both normal and derivative chromosomes. Metaphase FISH of lymphoblastoid cells derived from a t(2,3)-carrying family member localized breakpoints to a segment on chromosome 3 containing two genes and to a region on chromosome 2 lacking apparent genes (Fig. 2*A* and *B*). We next hybridized Southern blots containing restriction digested genomic DNA with probes from each of the

Author contributions: S.J.S., M.E.M., J.W., M.M.K., J.R.F., L.R.G., and M.S.H. designed research; S.J.S., M.E.M., J.W., M.M.K., Y.L., S.N., M.R., J.R.F., and M.S.H. performed research; G.B., T.K., K.O., H.L., P.H.W., M.R., M.L.M., M.T., J.R.F., and L.R.G. contributed new reagents/analytic tools; S.J.S., M.E.M., J.W., M.M.K., Y.L., S.N., L.R.G., and M.S.H. analyzed data; and M.S.H. wrote the paper.

The authors declare no conflict of interest.

This article is a PNAS Direct Submission.

[1]Present address: Perlegen Sciences, Mountain View, CA 94043.

[2]To whom correspondence should be addressed. E-mail: horwitz@u.washington.edu.

This article contains supporting information online at www.pnas.org/cgi/content/full/0904231106/DCSupplemental.

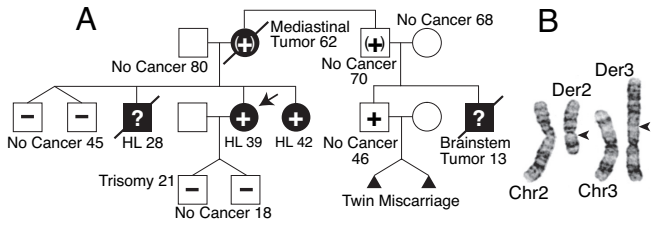

Fig. 1. Family inheriting cHL in association with constitutional, reciprocal t(2,3) chromosomal translocation. (*A*) Pedigree. Filled-in symbols represent individuals with cancer. Plus and minus signs denote those carrying, not carrying, (or inferred to carry), respectively, the translocation. For individuals with cancer, age of diagnosis (in years) is indicated; for those without cancer, present age is shown. Slash indicates individual is deceased. Question mark means translocation carrying status was not known before death and that archival material was unavailable. Arrow denotes proband. (*B*) Peripheral blood karyotype demonstrating translocation.

two genes from 3p21.31. One of them (*KLHDC8B*) yielded extra bands absent in an unaffected family member lacking the translocation (Fig. 2*C*), thus narrowing the interval to a region short enough to amplify by long-range PCR (Fig. 2*D*). We then progressively refined the interval by PCR (Fig. 2*E*) and used DNA sequencing to define precise breakpoints (Fig. 2*F*). The chromosome 3 breakpoint resides in the first intron of *KLHDC8B*. The chromosome 2 breakpoint is not located near known or hypothetical genes. Chromosomes 2 and 3 exhibit four base pairs of microhomology at the Der3 junction, and there is a four base pair nonhomologous insertion at the Der2 junction. We additionally excluded possible cryptic rearrangements by array-based comparative genomic hybridization. In sum, the translocation disrupts *KLHDC8B* and replaces sequences upstream of and including its first exon and part of its first intron with an intergenic region from chromosome 2, thus deleting its 5′-UTR and probable promoter sequences. Accordingly, quantitative real-time (QR) reverse transcription (RT)-PCR in lymphoblastoid cells shows that a translocation-carrying individual expresses only about half as much *KLHDC8B* as a family member without the translocation (Fig. 2*G*). Western blot confirms correspondingly reduced expression of protein, see below (Fig. 3*C*).

Association and Linkage with a *KLHDC8B* 5′-UTR Variant in Other cHL Pedigrees. We investigated whether mutations in this gene might occur in other cases of familial cHL. We screened probands from 52 families that each had two or more individuals affected with cHL. Sequencing of exons and adjacent regions, as well as copy number analysis, did not reveal any variants likely to alter protein coding or splicing. However, we did find a previously unreported single nucleotide polymorphism (SNP) in the 5′-UTR at +28 (with respect to transcription initiation). Heterozygous C→T substitution was present in affected probands from 3 of 52 (5.8%) cHL families, compared with just 4 of 307 controls (1.3%), yielding an odds ratio of 4.64 (95% confidence interval 1.01–21.4). Moreover, the variant segregates with cHL in each of these three pedigrees (Fig. 3*A*); of 13 individuals heterozygous for the C/T variant, seven have had cHL, whereas, of five individuals who are homozygous for the common allele (C/C), none have had any malignancy (nonparametric LOD = 1.20, $P <$ 0.01). The *KLHDC8B* variant therefore appears to be both associated and linked with cHL. Additionally, one C/T heterozygote has had lung cancer and two C/T heterozygotes have had both lung cancer and cHL. Of relevance, deletions of chromosome 3p21.3 are among the commonest and earliest known genetic alterations occurring in lung cancer (12).

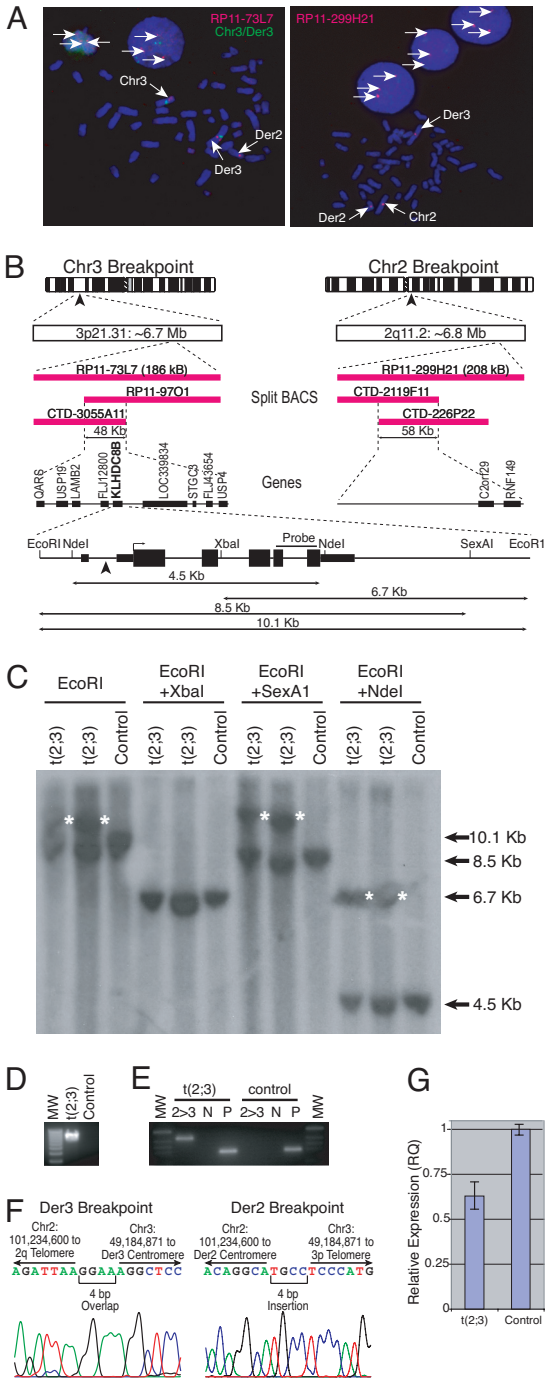

Fig. 2. Mapping the chromosomal translocation breakpoints. (*A*) FISH localizing translocation breakpoints to BAC clones RP11–73L7 from 3p21.31 and RP11–299H21 from 2q11.2 [labeled with rhodamine (red) along with chromosome 3 centromeric locator probe RP11–91A15 labeled with fluorescein (green)]. Arrows indicate split BAC hybridization signals. (*B*) Summary diagram of FISH mapping and Southern blot fine mapping strategy. (*C*) Southern blot of genomic DNA from two t(2,3) carriers and a control family member lacking the translocation, hybridized with a probe spanning *KLHDC8B* exons 5–6. Asterisks denote extra bands unique to translocation carriers. (*D*) Long-range PCR across t(2,3) breakpoint on Der3. MW, molecular weight marker. (*E*) PCR demonstrating ~350-bp fragment amplified across the Der3 breakpoint (''2 > 3'') from t(2,3) carrier, but not from control. ''P'' is positive control amplifiable from normal Chr3. ''N'' is negative control with primers on opposite sides of breakpoint. (*F*) Electropherograms crossing reciprocal breakpoints. Coordinates refer to human genome reference sequence hg18. (*G*) Taqman QR RT-PCR (repeated in triplicate) demonstrating *KLHDC8B* at approximately half normal mRNA levels in lymphoblastoid cells from t(2,3) carrier compared with control.

GENETICS

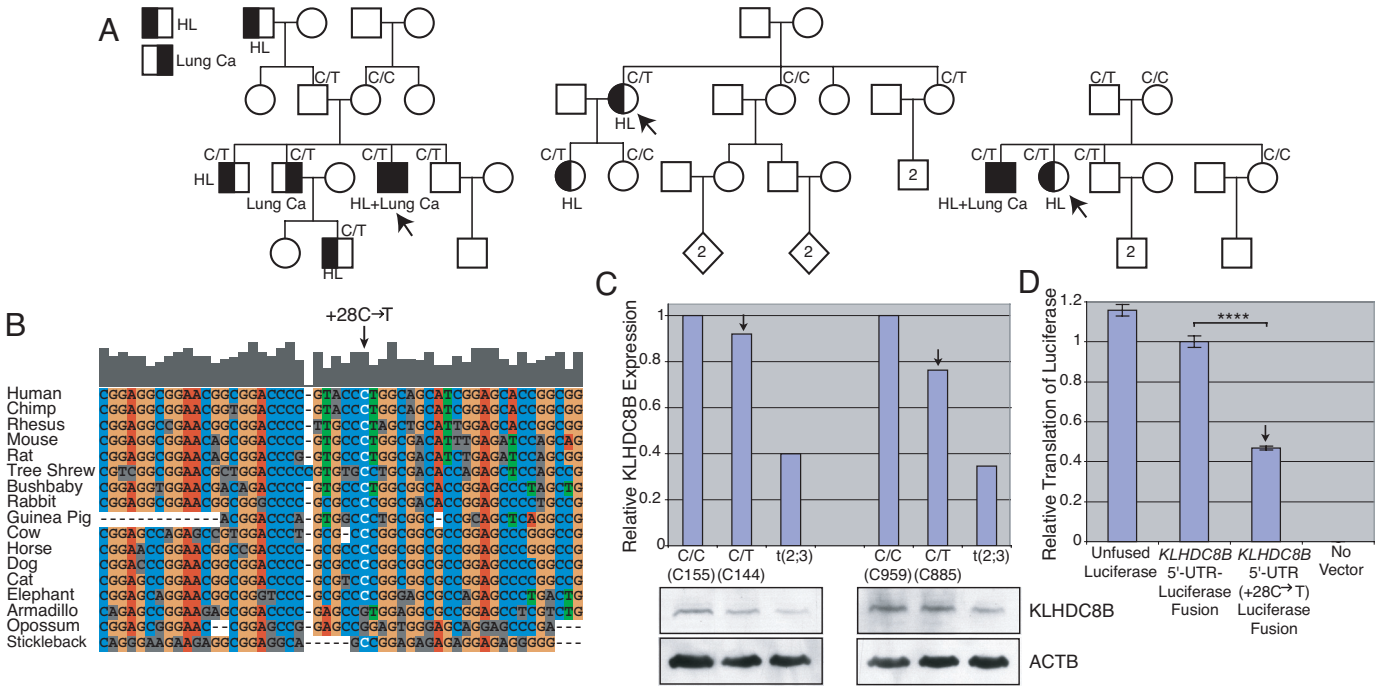

Fig. 3. Segregation of a 5′-UTR sequence variant with cHL and association with reduced amounts of KLHDC8B. (*A*) Three pedigrees in which heterozygosity for the variant (C/T) segregates with cHL. Arrows indicate probands. (*B*) Cross-species DNA sequence conservation at location of the 5′-UTR variant (+28C→T). Exon 1 alignment shown. (*C*) Reduced expression of KLHDC8B in two different sets of lymphoblastoid cells (numbers indicate ECACC cell lines) homozygous for the common allele (C/C) or heterozygous for the +28C→T variant (C/T) compared with t(2,3), as shown by western blot. Blot was probed with antibodies to β-actin (ACTB), as a loading control, and quantified by densitometry (Fig. S1). (*D*) Luciferase reporter assay showing that the +28C→T variant reduces translational efficiency. The 5′-UTR of *KLHDC8B*, with and without the C→T substitution, was fused to a firefly luciferase gene lacking an endogenous start codon, and tested compared with a positive control vector containing unfused firefly luciferase and a negative control transfection with *Renilla* luciferase vector alone. Shown is mean of three replicate assays for each of two transfections with standard error of the mean (SEM), all normalized to *Renilla* luciferase internal control. ****, $P < 10^{-4}$.

Translational Effect of the 5′-UTR Variant. The variant substitutes a highly conserved nucleotide residing in one of multiple poly(C) repeats in the 5′-UTR (Fig. 3*B*). To determine if this polymorphism influences expression, we performed Western blots on protein extracts from lymphoblastoid cells. Compared with those homozygous for the more common C-containing allele, in two different sets of people, heterozygosity for the +28C→T variant produces lower levels of KLHDC8B, although its effects are less pronounced than the translocation (Fig. 3*C* and Fig. S1). To determine how the variant influences expression, we first bacterially subcloned and sequenced cDNA from heterozygous lymphoblastoid cells, but found that each allele was represented in approximately equal proportions, excluding a transcriptional effect. To determine if the variant alters translation, we then evaluated expression in transfected HeLa cells using a recombinant reporter. We fused a portion of *KLHDC8B*, beginning from its 5′-UTR and extending six bases beyond the ATG initiation codon, in-frame to a luciferase gene lacking an initiation codon. The single base substitution at +28 reduces luciferase fusion gene expression by approximately half (Fig. 3*D*), demonstrating that the variant affects translation of the mRNA.

LOH for *KLHDC8B* in RS Cells. We then determined if *KLHDC8B* acquires somatic mutations in sporadic cases of cHL. Most lymphocytes contained within a Hodgkin lymphoma are reactive; malignant RS cells actually comprise just a minute fraction of the tumor (1). We therefore used fluorescence-activated cell sorting (FACS) to separate RS cells from reactive T and B cells in tumors obtained from six cHL patients. We did not detect any DNA sequence alterations in genomic DNA from transcribed regions of the gene in RS cells. We next assayed for possible LOH as an indication of somatic deletion or gene conversion events. RS cells isolated from the tumor of one patient demonstrated LOH for five SNPs from within and flanking *KLHDC8B* (Fig. 4 and Dataset S1). RS cells from another two patients each demonstrated heterozygosity for different informative SNPs from within *KLHDC8B* (Dataset S1), indicating that LOH was unlikely (although a small region of LOH cannot be excluded). For the remaining three patients, no informative SNPs could be identified (Dataset S1). Thus, out of three informative sporadic

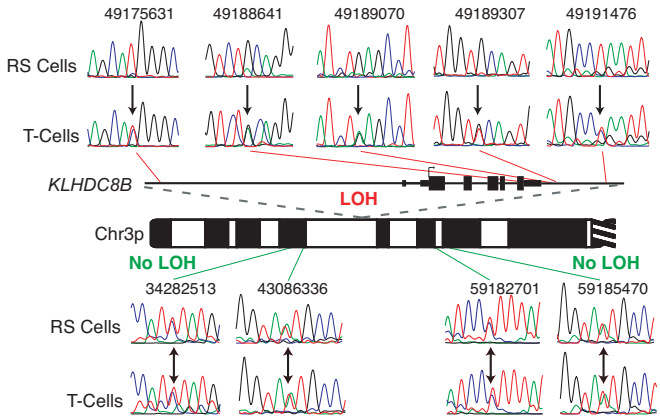

Fig. 4. LOH in region of 3p21.31 containing *KLHDC8B* in RS cells from sporadic cHL case, showing electropherograms for informative (heterozygous) SNPs contrasted between tumor-derived RS and reactive T cells. Coordinates refer to human genome reference sequence hg18.

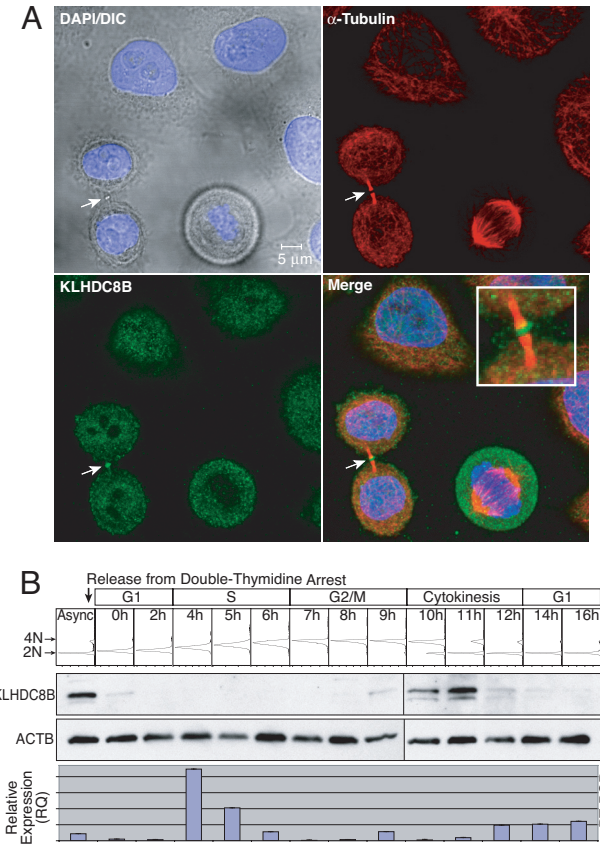

Fig. 5. Midbody localization and cell cycle-specific transcription and translation of KLHDC8B. (*A*) Confocal microscopy of indirect immunofluorescence for KLHDC8B (green) and α-tubulin (red) and DAPI-counterstained nuclei (blue) in unsynchronized HeLa cells. Left two panels show a single plane through the midbody; right two panels are projections of five adjacent planes. DIC, differential interference contrast. Arrows point to midbody (enlarged in *Inset*). (*B*) HeLa cells were released from double-thymidine block, collected at intervals, and each time-point analyzed by flow cytometry, western blot of KLHDC8B with ACTB as loading control, and TaqMan QR RT-PCR of *KLHDC8B* repeated in quadruplicate.

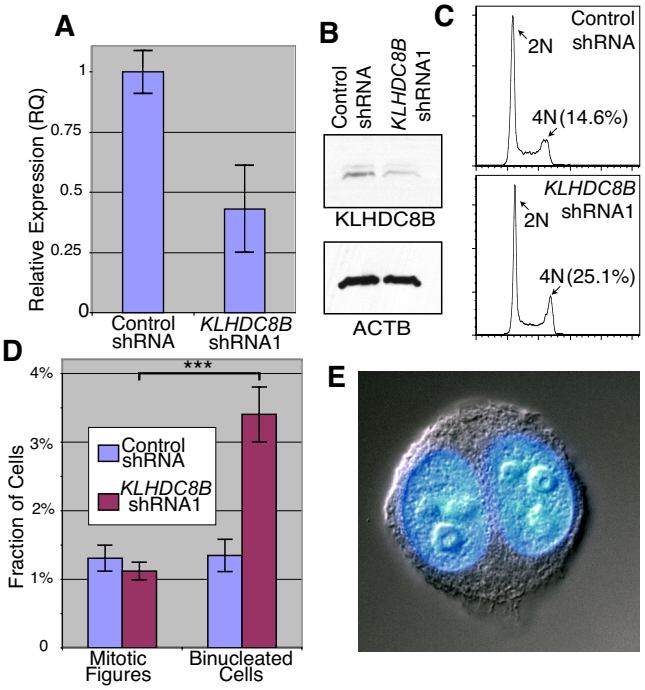

Fig. 6. Increase in binucleated cells after KLHDC8B depletion. (*A*) *KLHDC8B* shRNA reduces levels of transcript, as measured by TaqMan QR RT-PCR in HeLa cells. (*B*) *KLHDC8B* shRNA reduces levels of protein, as measured by western blot in HeLa cell extracts. Western blot was probed with antibodies to ACTB, as a loading control. (*C*) shRNA-mediated reduction of KLHDC8B increases proportion of HeLa cells with 4N DNA content. (*D*) Proportion of cells in mitosis is unchanged, but number of binucleated cells is increased after shRNA-mediated reduction of KLHDC8B. Results of manual counting of cells treated with either control or *KLHDC8B*-specific shRNA; error bars correspond to the SEM for nine replicates, in which batches of ~250 cells under each condition were counted, in two separate transfections (replicates 1–2 and 3–9) performed on separate days. ***, $P < 0.001$. (*E*) Example of binucleated HeLa cell after *KLHDC8B* shRNA treatment, DIC image of DAPI-stained nuclei.

cHL patients, RS cells from one demonstrated LOH in a region of 3p21.21 including *KLHDC8B*.

Localization of KLHDC8B at the Midbody. *KLHDC8B* is a widely expressed (per publicly available databases) yet previously uncharacterized gene predicted to encode a protein consisting of nothing but seven kelch domains (13), which fold into β-propeller structures capable of participating in protein-protein interactions (13). Kelch repeat-containing proteins comprise a large family with diverse activities (13). To characterize its function, we generated antibodies to KLHDC8B and evaluated its subcellular distribution by immunofluorescent staining of HeLa cells (where our preliminary studies showed it is also transcribed). KLHDC8B accumulates most strongly in mitotic cells and concentrates in the midbody of the cytoplasmic bridge linking daughter cells as they are about to separate during cytokinesis (Fig. 5*A* and Fig. S2). To determine if *KLHDC8B* expression is cell cycle-regulated, we synchronized HeLa cells at G1 by release from a double-thymidine block and collected fractions at successive time points. Flow cytometry, western blot, and QR RT-PCR demonstrate that *KLHDC8B* is transcribed predominantly during S phase, translated exclusively during mitosis and cytokinesis (when the 4N population is transitioning to 2N), and is rapidly degraded after cell division (Fig. 5*B*). Based on its timing and location of expression, KLHDC8B appears to be involved in cytokinesis.

Binucleation After Depletion of KLHDC8B. In general, when cytokinesis fails, the cleavage furrow regresses, resulting in binucleated cells (14). To determine if loss of KLHDC8B can disrupt cytokinesis and cause binucleation, we used RNA interference to deplete its expression in HeLa cells. Flow cytometry demonstrates that reducing KLHDC8B expression to about half normal level [as measured by QR RT-PCR (Fig. 6*A*), and western blot (Fig. 6*B*)], yields an increased proportion of cells with 4N DNA content (Fig. 6*C*). We then microscopically examined shRNA-treated cells and found that, whereas the overall proportion of cells engaged in mitosis is unchanged, there is an increased frequency of binucleated cells (Fig. 6 *D* and *E*). As a control for off-target effects of RNAi, we tested two additional shRNAs and found that each elevated binucleated cell production in relation to how well it functioned in silencing *KLHDC8B* (Fig. S3). Finally, we tested whether we could complement RNAi's effect on binucleation by expressing an RNAi-resistant form of *KLHDC8B*. We cotransfected siRNA targeting either the 5′- or 3′-UTR of the endogenous gene along with cDNA correspondingly lacking either only the 5′- or 3′-UTR (Fig. S4). Compared with a control expressing β-galactosidase, the cDNA missing only the 3′-UTR indeed reversed binucleation resulting from the siRNA targeting the 3′-UTR, whereas the cDNA lacking the 5′-UTR (which still contains the 3′-UTR and should remain

vulnerable to siRNA targeting the 3′-UTR) did not. For the siRNA targeting the 5′-UTR of *KLHDC8B*, the construct lacking only the 3′-UTR did not complement binucleation, as expected; however, cDNA deleted of its 5′-UTR could not fully complement the binucleation defect. The most likely explanation for the latter is that the 5′-UTR of *KLHDC8B* is necessary for its appropriate function in cytokinesis—an interpretation consistent with the observed effects of genetic variants in the 5′-UTR in familial cHL. Reduced expression of KLHDC8B leads to formation of binucleated cells, thus recapitulating a hallmark of cHL.

Discussion

We discovered a constitutional translocation disrupting transcription of *KLHDC8B* in a family with multiple cases of cHL. In the general population, 0.29–0.56% carries a balanced translocation, but, because relatively little of the genome encodes genes, only very few translocations actually interrupt genes (15). Moreover, among lymphocytes, *KLHDC8B* is expressed most strongly in germinal center B cells (16), which are the malignant cell of origin for cHL. The translocation seems unlikely to be only coincidentally related to cHL in this family.

Additionally, we found that a 5′-UTR variant that reduces *KLHDC8B* translation is associated with familial cHL and linked to disease in three other families. The 5′-UTR variant is located within a poly(C) repeat cluster. RNA-binding, KH domain-containing proteins recognize poly(C) repeats (17) and participate in cap-independent translation (18). Significantly, *KLHDC8B* is translated only during mitosis and cytokinesis, when cap-dependent translation is extinguished and only cap-independent translation is available (19). The 5′-UTR variant may therefore disrupt *KLHDC8B*'s mitotic expression. More studies are needed, however, to determine if this variant acts as a causative mutation or whether it might modify risk for developing cHL or other cancers in concert with other genetic and environmental factors.

RS cells from one of three informative sporadic cases of cHL demonstrate LOH for *KLHDC8B*. Although intriguing, the extent of LOH remains large, and we were unable to obtain sufficient material to evaluate for additional genetic alterations. The contribution of somatic mutations of *KLHDC8B* to sporadic cHL requires further study.

The kelch domain was initially discovered as a repeated element in an oligomeric actin-organizing *Drosophila* protein serving as a component of "ring canals," which are structures that interconnect germ cells remaining physiologically coupled after incomplete cytokinesis (20). Other kelch proteins also participate in cytokinesis. Coiled-coil kelch proteins Kel1p and Kel2p (21) and Tea1p (22) function to correctly position the bud neck and cell division plane, respectively, in budding and fission yeast. The mammalian BTB/POZ-kelch protein, Keap1, which has a more well-established role in coordinating response to oxidative stress via recruitment of cullin E3 ubiquitin ligase (Cul3) to the transcription factor Nrf2 (23), is one of just a few proteins that, like KLHDC8B, are known to locate to the midbody's central matrix (24). Recently, two more BTB/POZ-kelch proteins, KLHL9 and KLHL13, were discovered in the midbody, where they associate with the Aurora kinase spindle checkpoint regulator and also direct its ubiquitination by Cul3 (25). Silencing of Keap1 (24), KLHL9 (25), and KLHL13 (25) similarly increases binucleated cell formation. Another BTB/POZ-kelch protein, Nd1, participates in cytoskeletal organization, and overexpression retards cytokinesis (26).

Most provocatively, the binucleated RS cell of cHL forms as a consequence of defective cytokinesis (27), rather than through cell fusion (28), and we demonstrate that KLHDC8B participates in cytokinesis, where its reduced expression leads to formation of binucleated cells. Overall, our observations are consistent with a hypothesis, originally formulated nearly a century ago by Boveri, that defective cytokinesis promotes tumorigenesis through the formation of genetically unstable tetraploid cells (29). An implication is that other midbody proteins may prove to represent a general class of tumor suppressors. Supportive observations include recent demonstrations that somatic mutations of *KEAP1* are frequent in lung cancer (30) and that BRCA1 (31), BRCA2 (32), and BRCA1-associated protein BARD1 (33), in addition to other important contributions to cancer, also each locate to the midbody during cytokinesis.

Materials and Methods

Cases and Controls. Cases were recruited under Human Subjects Committee-approved protocols. Control individual genomic DNA and lymphoblastoid cell lines were obtained (via Sigma-Aldrich) from the European Collection of Animal Cell Cultures (ECACC).

FISH. BAC clones were provided by the Children's Hospital of Oakland Research Institute BACPAC Resource Center. BACS were labeled with a nick translation kit (Roche) using fluorescein-12-dUTP or tetramethyl-rhodamine-6-dUTP. Hybridization was performed as described (34).

Purification of RS Cells. RS and nonmalignant reactive lymphocytes were purified from lymph node suspensions via flow cytometric cell sorting using a mixture of antibodies (35).

Mutational Analysis. We performed DNA sequencing with the ABI BigDye Terminator v3.1 Cycle Sequencing kit (Applied Biosystems). We screened all six *KLHDC8B* exons and intron-exon junctions. To evaluate copy number variation, we additionally performed exonic multiplex ligation-dependent probe amplification using SALA MLPA reagent kits (MRC-Holland). For LOH analysis, we selected known SNPs from dbSNP (http://www.ncbi.nlm.nih.gov/projects/SNP) and sequenced KLHDC8B introns in sporadic cHL cases to search for previously unreported SNPs.

Statistics. The association between the 5′-UTR variant and cHL was calculating using the odds ratio (36). The nonparametric LOD score for segregation of the 5′-UTR variant within families was calculated using the Kong and Cox exponential model (37), with observed allele frequencies for cases and controls, using the MERLIN software package (38). *P* values for luciferase and shRNA assays derive from two-tailed, two-sample T-tests assuming equal variances.

Quantitative RT-PCR. Total RNA was prepared from lymphoblastoid or HeLa (obtained from ATCC) cells using the Absolutely RNA Miniprep kit (Stratagene) and used to produce randomly primed cDNAs with the Omniscript RT kit (Qiagen). QR RT-PCR was performed using an ABI 7300 real-time PCR system (Applied Biosystems). *KLHDC8B* TaqMan gene expression assays (HS00293902 m1) were obtained from Applied Biosystems and normalized to *ACTB*, encoding β-actin.

Luciferase Assays. We fused the *KLHDC8B* 5′-UTR extending downstream to the third amino acid residue of its protein coding sequence in-frame to the second amino acid residue of firefly luciferase (deleting the endogenous translation initiation codon in luciferase) in the pPK-CMV-CLuc Stable Fusion Protein Reporter Vector (PromoKine) and introduced the +28C→T variant by site-directed mutagenesis. Each of the wild-type and variant firefly luciferase fusion construct plasmids (3.75 μg) was transfected with Lipofectamine (Invitrogen) along with 0.25 μg pRL-TK *Renilla* luciferase as internal control in ~80% confluent HeLa cells on 10-cm plates and assayed 24 h later using the Promega Dual-Luciferase Reporter Assay System.

Antibodies, Immunofluorescence, and Western Blotting. Chicken polyclonal IgY antibodies were raised (by Aves Labs) against KLHDC8B peptide $_{138}$DTAPQAQVRVYEPRRDC$_{154}$. (Negative controls included preimmune and antigen-depleted sera.) Immunofluorescent staining of HeLa cells, fixed in 4% paraformaldehyde and permeabilized with 0.1% Triton X-100, used a 1:10,000 dilution of α-KLHDC8B and 1:500 dilution of α-tubulin (ab7291; Abcam) primary antibodies followed with a 1:500 dilution of Alexa Fluor 488-labeled goat anti-chicken and 1:500 Alexa 555-labeled goat anti-mouse secondary antibodies (Invitrogen), blocked with 0.5% BSA and 4′,6-diamino-2-phenylindole (DAPI) nuclear counterstaining. Images were obtained with a Zeiss 510 laser-scanning confocal microscope with 63× Plan-Apochromat

objective using Zeiss LSM Image Browser software. Cell extracts were prepared with the Complete Lysis-M kit (Roche). Western blots used a 1:10,000 dilution of primary antibody followed with a 1:10,000 dilution of Aves Labs horseradish peroxidase (HRP)-conjugated goat anti-chicken IgY secondary antibody, developed with the ECL Western Blotting Detection kit (Amersham). Actin loading control was detected with the C-11 HRP-conjugated antibody (Santa Cruz Biotechnology). Densitometry used ImageJ software [Wayne Rasband, National Institutes of Health (NIH)] analysis of scanned BioMax Light (Kodak) film.

RNA Interference and Cell Cycle Analysis. One microgram *KLHDC8B* shRNA plasmid vectors TI369558 (''shRNA1''), TI369557 (''shRNA2''), TI369559 (''shRNA3''), and noneffective GFP negative control vector TR30003 (Origene) were individually transfected into ~90% confluent HeLa cells on six-well plates using Lipofectamine Plus (Invitrogen). Cells were split to ~10% confluency 24 h after transfection and then harvested an additional 16 h later for protein extraction for Western blot, RNA extraction for RT-PCR, and propidium iodide staining of ethanol-fixed RNase A-treated cells for cell cycle analysis, performed on a BD FACSCanto flow cytometer. shRNA-treated cells were also plated on coverslips and stained with DAPI to manually count (25) the proportion of mitotic figures and binucleated cells. Custom siRNA (25 pg) targeting 5′- and 3′-UTRs (Fig. S4) or Silencer Negative Control #1 siRNA (Ambion) were transfected with 1 μg pCS2+ vector (39) expressing full-length *KLHDC8B*, *KLHDC8B* from which either the 5′- or 3′-UTR was deleted, or a β-galactosidase gene, as a control, into ~90% confluent HeLa cells on six-well plates using Lipofectamine Plus (Invitrogen). Cells exposed to *KLHDC8B*-specific or control RNAi were split to ~10% confluency 24 h after transfection and scored an additional 24 h later by systematically moving the microscope stage. HeLa cells were synchronized via double-thymidine block (40), except that thymidine concentration was increased to 2.5 mM.

ACKNOWLEDGMENTS. We thank participating families, W. Raskind and J. Wolff for EBV transformation of lymphoblasts, H. Massa and B. Trask for instruction in FISH, and T. Drumheller for case referral. This work was supported by the University of Washington Medical Scientist Training Program and National Institutes of Health Grant F30AG030316 (to S.J.S.); Doris Duke Charitable Foundation Clinical Scientist Development Award (M.E.M.); Fred Hutchinson/UW Cancer Consortium's Cancer Center Support Grant (M.S.H.); and Intramural Research Program of the National Institutes of Health, National Cancer Institute, Division of Cancer Epidemiology and Genetics, and contract N02-CP-55506 (to M.L.M., M.T., and L.R.G.).

1. Re D, Thomas RK, Behringer K, Diehl V (2005) From Hodgkin disease to Hodgkin lymphoma: Biologic insights and therapeutic potential. *Blood* 105:4553–4560.
2. Kutok JL, Wang F (2006) Spectrum of Epstein-Barr virus-associated diseases. *Annu Rev Pathol* 1:375–404.
3. Goldin LR, et al. (2004) Familial aggregation of Hodgkin lymphoma and related tumors. *Cancer* 100:1902–1908.
4. Goldin LR, et al. (2005) A genome screen of families at high risk for Hodgkin lymphoma: Evidence for a susceptibility gene on chromosome 4. *J Med Genet* 42:595–601.
5. Sparkes RS, Muller H, Klisak I (1979) Retinoblastoma with 13q- chromosomal deletion associated with maternal paracentric inversion of 13q. *Science* 203:1027–1029.
6. Kinzler KW, et al. (1991) Identification of FAP locus genes from chromosome 5q21. *Science* 253:661–665.
7. Szeles A (2002) Fluorescence in situ hybridization (FISH) in the molecular cytogenetics of cancer. *Acta Microbiol Immunol Hung* 49:69–80.
8. Xiong W, et al. (2004) A susceptibility locus at chromosome 3p21 linked to familial nasopharyngeal carcinoma. *Cancer Res* 64:1972–1974.
9. Cheng Y, et al. (1998) Functional evidence for a nasopharyngeal carcinoma tumor suppressor gene that maps at chromosome 3p21.3. *Proc Natl Acad Sci USA* 95:3042–3047.
10. Chan AS, et al. (2000) High frequency of chromosome 3p deletion in histologically normal nasopharyngeal epithelia from southern Chinese. *Cancer Res* 60:5365–5370.
11. Yang Q, et al. (2002) Chromosome 3p and breast cancer. *J Hum Genet* 47:453–459.
12. Hesson LB, Cooper WN, Latif F (2007) Evaluation of the 3p21.3 tumour-suppressor gene cluster. *Oncogene* 26:7283–7301.
13. Prag S, Adams JC (2003) Molecular phylogeny of the kelch-repeat superfamily reveals an expansion of BTB/kelch proteins in animals. *BMC Bioinformatics* 4:42.
14. Glotzer M (2005) The molecular requirements for cytokinesis. *Science* 307:1735–1739.
15. Pickard BS, et al. (2005) Cytogenetics and gene discovery in psychiatric disorders. *Pharmacogenomics J* 5:81–88.
16. Luckey CJ, et al. (2006) Memory T and memory B cells share a transcriptional program of self-renewal with long-term hematopoietic stem cells. *Proc Natl Acad Sci USA* 103:3304–3309.
17. Thisted T, Lyakhov DL, Liebhaber SA (2001) Optimized RNA targets of two closely related triple KH domain proteins, heterogeneous nuclear ribonucleoprotein K and alphaCP-2KL, suggest Distinct modes of RNA recognition. *J Biol Chem* 276:17484–17496.
18. Le Breton M, et al. (2005) Translational control during mitosis. *Biochimie* 87:805–811.
19. Wilker EW, et al. (2007) 14–3-3sigma controls mitotic translation to facilitate cytokinesis. *Nature* 446:329–332.
20. Xue F, Cooley L (1993) kelch encodes a component of intercellular bridges in *Drosophila* egg chambers. *Cell* 72:681–693.
21. Chang F, Feierbach B, Martin S (2005) Regulation of actin assembly by microtubules in fission yeast cell polarity. *Novartis Found Symp* 269:59–66.
22. Knaus M, et al. (2005) The Bud14p-Glc7p complex functions as a cortical regulator of dynein in budding yeast. *EMBO J* 24:3000–3011.
23. Kobayashi A, et al. (2004) Oxidative stress sensor Keap1 functions as an adaptor for Cul3-based E3 ligase to regulate proteasomal degradation of Nrf2. *Mol Cell Biol* 24:7130–7139.
24. Skop AR, et al. (2004) Dissection of the mammalian midbody proteome reveals conserved cytokinesis mechanisms. *Science* 305:61–66.
25. Sumara I, et al. (2007) A Cul3-based E3 ligase removes Aurora B from mitotic chromosomes, regulating mitotic progression and completion of cytokinesis in human cells. *Dev Cell* 12:887–900.
26. Sasagawa K, et al. (2002) Identification of Nd1, a novel murine kelch family protein, involved in stabilization of actin filaments. *J Biol Chem* 277:44140–44146.
27. Leoncini L, et al. (1997) Cell kinetics, morphology, and molecular IgVH gene rearrangements in Hodgkin's disease. *Leuk Lymphoma* 26:307–316.
28. Kuppers R, et al. (2001) Evidence that Hodgkin and Reed-Sternberg cells in Hodgkin disease do not represent cell fusions. *Blood* 97:818–821.
29. Barr FA, Gruneberg U (2007) Cytokinesis: Placing and making the final cut. *Cell* 131:847–860.
30. Ohta T, et al. (2008) Loss of Keap1 function activates Nrf2 and provides advantages for lung cancer cell growth. *Cancer Res* 68:1303–1309.
31. Lotti LV, et al. (2002) Subcellular localization of the BRCA1 gene product in mitotic cells. *Genes Chromosomes Cancer* 35:193–203.
32. Daniels MJ, Wang Y, Lee M, Venkitaraman AR (2004) Abnormal cytokinesis in cells deficient in the breast cancer susceptibility protein BRCA2. *Science* 306:876–879.
33. Ryser S, et al. (2009) Distinct roles of BARD1 isoforms in mitosis: Full-length BARD1 mediates Aurora B degradation, cancer-associated BARD1beta scaffolds Aurora B and BRCA2. *Cancer Res* 69:1125–1134.
34. Trask BJ (1991) DNA sequence localization in metaphase and interphase cells by fluorescence in situ hybridization. *Methods Cell Biol* 35:3–35.
35. Fromm JR, Kussick SJ, Wood BL (2006) Identification and purification of classical Hodgkin cells from lymph nodes by flow cytometry and flow cytometric cell sorting. *Am J Clin Pathol* 126:764–780.
36. Bland JM, Altman DG (2000) Statistics notes. The odds ratio. *BMJ* 320:1468.
37. Kong A, Cox NJ (1997) Allele-sharing models: LOD scores and accurate linkage tests. *Am J Hum Genet* 61:1179–1188.
38. Abecasis GR, Cherny SS, Cookson WO, Cardon LR (2002) Merlin—rapid analysis of dense genetic maps using sparse gene flow trees. *Nat Genet* 30:97–101.
39. Turner DL, Weintraub H (1994) Expression of achaete-scute homolog 3 in *Xenopus* embryos converts ectodermal cells to a neural fate. *Genes Dev* 8:1434–1447.
40. Whitfield ML, et al. (2000) Stem-loop binding protein, the protein that binds the 3′ end of histone mRNA, is cell cycle regulated by both translational and posttranslational mechanisms. *Mol Cell Biol* 20:4188–4198.